Chin. Geogra. Sci. 2015 Vol. 25 No. 3 pp. 295–308
doi: 10.1007/s11769-014-0690-5

Springer Science Press
www.springerlink.com/content/1002-0063

Spectral Characterization of Colored Dissolved Organic Matter for Productive Inland Waters and Its Source Analysis

SONG Kaishan[1, 2], LI Lin[1], Lenore TEDESCO[3], Nicolas CLERCIN[1], LI Linhai[1], SHI Kun[1]

(1. *Department of Earth Sciences*, *Indiana University-Purdue University*, *Indianapolis* 46202, *US*; 2. *Northeast Institute of Geography and Agroecology*, *Chinese Academy of Sciences*, *Changchun* 130102, *China*; 3. *The Wetlands Institute*, *Stone Harbor*, *New Jersey* 08247, *US*)

Abstract: This study examined the spatiotemporal dynamics of colored dissolved organic matter (CDOM) and spectral slope (*S*), and further to analyze its sources in three productive water supplies (Eagle Creek, Geist and Morse reservoirs) from Indiana, USA. The results showed that he absorption coefficient $a_{CDOM}(440)$ ranged from 0.37 m^{-1} to 3.93 m^{-1} with an average of 1.89 ± 0.76 m^{-1} (±SD) for the aggregated dataset, and *S* varied from 0.0048 nm^{-1} to 0.0239 nm^{-1} with an average of 0.0108 ± 0.0040 nm^{-1}. A significant relationship between *S* and $a_{CDOM}(440)$ can be fitted with a power equation ($S = 0.013 \times a_{CDOM}(440)^{-0.42}$, $R^2 = 0.612$), excluding data from Geist Reservoir during high flow (12 April 2010) and the Morse Reservoir on 25 June 2010 due to a T-storm achieves even higher determination coefficient ($R^2 = 0.842$). Correlation analysis indicated that $a_{CDOM}(440)$ has strong association with inorganic suspended matter (ISM) concentration ($0.231 < R^2 < 0.786$) for each of the field surveys, and this trend followed the aggregated datasets ($R^2 = 0.447$, $p < 0.001$). In contrast, chlorophyll-a was only correlated with $a_{CDOM}(440)$ in summer and autumn ($0.081 < R^2 < 0.763$), indicating that CDOM is mainly from terrigenous sources in early spring and that phytoplankton contributed during the algal blooming season. The *S* value was used to characterize CDOM origin. The results indicate that the CDOM source is mainly controlled by hydrological variations, while phytoplankton originated organic matter also closely linked with CDOM dynamics in three productive reservoirs.

Keywords: absorption coefficient; colored dissolved organic matter (CDOM); chlorophyll-a; spectral slope (*S*); inorganic suspended matter (ISM)

Citation: Song Kaishan, Li Lin, Tedesco Lenore, Clercin Nicolas, Li Linhai, Shi Kun, 2015. Spectral characterization of colored dissolved organic matter for productive inland waters and its source analysis. *Chinese Geographical Science*, 25(3): 295–308. doi: 10.1007/ s11769-014-0690-5

1 Introduction

Colored dissolved organic matter (CDOM) is an important component that governs light propagation in waters (Miller *et al*., 2009; Zhang *et al*., 2011a). The CDOM mainly originates from terrestrial input or phytoplankton decomposition, which primarily consists of dissolved organic carbon (DOC) in the form of fulvic or humic acids (Wetzel, 2001). The CDOM absorbs short-wavelength light (ultraviolet and blue) and leaves water a yellow or tea-stained color (Bricaud *et al*., 1981; Williamson and Rose, 2010). It influences light attenuation in both inland and open waters (Vodacek *et al*., 1997; Zhang *et al*., 2007), which affects the transport and bio-availability of materials, such as trace metals and organic pollutants (Wetzel, 2001; Helms *et al*., 2013a). The CDOM is a source of nutrients and energy for heterotrophic bacteria, and serves to mediate the chemical environment through the production of organic acids (Babin *et al*., 2003; Helms *et al*., 2008; 2013b) and to

Received date: 2013-02-27; accepted date: 2013-05-28
Foundation item: Under the auspices of National Aeronautics and Space Administration of US (NASA) (No. NNG06GA92G), National Natural Science Foundation of China (No. 41171293)
Corresponding author: SONG Kaishan. E-mail: songks@iga.ac.cn

enhance or alleviate the toxic forms of heavy metals, e.g., aluminum or mercury (Cory *et al*., 2006).

The CDOM concentration is defined optically in terms of the absorption unit of sample filtrates (Bricaud *et al*., 1981; Babin *et al*., 2003), and sometimes reported as DOC (Busse and Gunkel, 2001, Fichot and Benner, 2011). The composition of CDOM affects the absorption characteristic along wavelength (Carder *et al*., 1989; Helms *et al*., 2008; Spencer *et al*., 2012). Spectral slope (*S*) provides information on CDOM origins, chemical process and diagenesis. The merit of application of *S* lies on its independence upon CDOM concentration (Twardowski *et al*., 2004; Helm *et al*., 2008; Spencer *et al*., 2009). The *S* has been used for correcting bio-optical models (Lee *et al*., 2002) and monitoring CDOM degradative processes (Hu *et al*., 2006; Morel and Gentili, 2009; Spencer *et al*., 2012). Carder *et al*. (1989) reported that *S* value may be used as a proxy to quantify the ratio of fulvic acids to humic acid. It also has been proven that *S* strongly correlates with fulvic acid molecular weight (Carder *et al*., 1989; Helms *et al*., 2008; Jaffe *et al*., 2008). So far, different curve fitting methods used (e.g., linear fitting-based logarithmic transform or direct exponential curve fitting) or various spectral wavelength ranges considered, e.g., 280–310 nm in Brown (1977), 350–500 nm in Bricaud *et al*. (1981), 300–650 nm in Stedmon *et al*. (2006), and other ranges (Twardowski *et al*., 2004, and therein) lead to various predicted CDOM and *S*.

Transformations of CDOM, the absorbing component of dissolved organic matter (DOM) in natural waters, are expected to have a significant impact on carbon cycling dynamics (Jaffe *et al*., 2008; Spencer *et al*., 2009; Tranvik *et al*., 2009). A preliminary inventory of CDOM absorptions in the ultraviolet (UV) and visible spectral regions as well as their spatiotemporal characteristics linking to phytoplankton and suspended mineral in productive inland waters have not yet been widely conducted (Binding *et al*., 2008; Zhang *et al*., 2009; 2011a; Song *et al*., 2010), which merits further investigations. In the present study, we examine the optical properties of CDOM and the factors that affect these properties in three productive inland waters. The CDOM optical properties and their association with chlorophyll-a (Chl-a) and inorganic suspended matter (ISM) are examined in three productive reservoirs in the central Indiana, USA due to the coating effect. The aims are to investigate 1) the spatiotemporal characteristics of CDOM and *S* value, and 2) the process that controls CDOM origin and spatiotemporal patterns in productive inland waters in agriculturally dominant watersheds through absorbance analysis, particularly in algal blooming seasons.

2 Materials and Methods

2.1 Study sites

The present study is focused on three potable water supply sources located in the central Indiana (Fig. 1), i.e., the Eagle Creek Reservoir (ECR: surface area (A) = 5.0 km^2; mean depth (Z) = 4.2 m), the Geist Reservoir (GR: A = 7.5 km^2; Z = 3.2 m), and Morse Reservoir (MR: A = 6.0 km^2; Z = 4.7 m), with average water residence times of 56 d, 55 d and 70 d, respectively. The ECR is fed by a 420 km^2 watershed dominated by agricultural land (60.1%) with some sub-watersheds transitioning to sub-urban development. The GR is fed by the 567 km^2 Fall Creek watershed with 60.0% of agricultural land. The MR is fed by the 554 km^2 Cicero Creek watershed, where 76.9% is agricultural land. Forest buffer zones surround both the ECR and GR (Fig. 1). The water quality in these reservoirs is impaired due to high nutrient concentrations, which result in nuisance summer algal blooms (Song *et al*., 2013). Snow cover is highly variable in central Indiana with pulses of watershed inflows into the reservoirs associated with winter storms and punctuated snowmelt and winter rain events. Rain on snow events or punctuated warm periods throughout the winter result in flooding and transport of soil and residual agriculturally sourced carbon from bare ground areas.

2.2 Water quality determination

Ten field surveys were conducted from April 12 to October 21, 2010. Surface mixing water samples were collected at each sampling station from three depths at approximately 0.25 m, 0.50 m, and 1.00 m below the water surface. Samples were analyzed in the laboratory for Chl-a, total suspended matter (TSM), and inorganic suspended matter ISM. The Chl-a concentration was determined fluorometrically by using a TD-700 Fluorometer (Turner Designs, CA) following Arar and Collins (1997). The TSM was determined gravimetrically. The filters used to measure the TSM were weighed and then ashed for 75 min at 550℃ in porcelain muffle furnace to determine ISM, the methods for both TSM and ISM are detailed in Song *et al*. (2012). Turbidity was determined

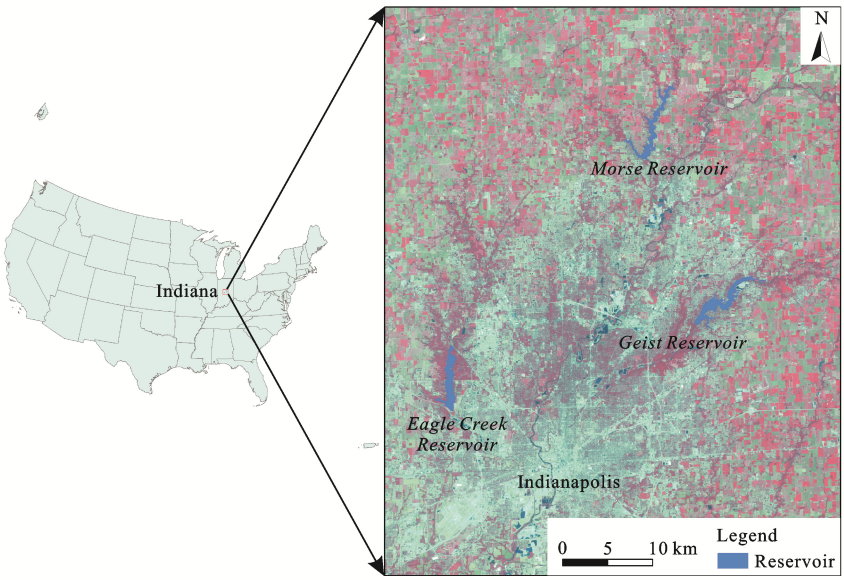

Fig. 1 Location of three reservoirs (Eagle Creek Reservoir, Morse Reservoir and Geist Reservoir) in central Indiana, USA

using YSI 600 XLM portable probe (YSI Inc., Yellow Springs, OH).

2.3 Phytoplankton identification and enumeration

Weekly water samples near each reservoir dam were collected for cyanobacteria identification and cell counting during 2008–2010 by Center of Earth and Environmental Science (CEES) at Indiana University-Purdue University, Indianapolis (Song *et al*., 2013). Subsamples of 50 mL of the surface (–0.25 m) grab sample were fixed with Lugol′s iodine solution and stored in the dark at 4℃ for phytoplankton analyses. All samples were examined using a Nikon Optiphot-Pol microscope for phytoplankton identification and enumeration. The enumeration of the most common genera and/or species was carried out at a magnification range of 200–400 using a Nageotte counting chamber. Cyanobacteria cells were counted in a Nageotte cell (50 μL) which is efficient at mitigating the flotation of phytoplankton caused by gas-filled vesicles. The number of stripes counted was determined when the number of colonies or dominant filaments was higher than 40 (Tedesco and Clercin, 2011). When this number fell below the threshold of 40 stripes, allowing estimation in the counting chamber, the sample was concentrated by filtration (25–100 mL) on a laser-perforated polycarbonate membrane (1 μm pore size). The filtrate was recovered by friction in 1 mL and then mixed to be injected into the Nageotte cell. Biovolumes were calculated from recorded abundances and specific biovolume approximations to simple geometrical shapes (Sun and Liu, 2003).

2.4 CDOM absorption determination

In the laboratory, the samples were filtered at low pressure using Millipore membrane cellulose filters with a 0.22 μm pore size. Absorption spectra were obtained between 280 nm and 800 nm at 1 nm increments using a Shimadzu UV-2550PC UV-Vis dual beam spectrophotometer through a 1 cm quartz cuvette. Milli-Q water was used as reference. The absorption coefficient a_{CDOM} was calculated from the measured optical density (OD) of the sample using Equation (1):

$$a_{\mathrm{CDOM}}(\lambda) = 2.303[OD_{\mathrm{S}(\lambda)} - OD_{(\mathrm{null})}] / \gamma \quad (1)$$

where γ is the cuvette path length (0.01 m) and 2.303 is the conversion factor of base 10 to base e (2.718) logarithms. Some fine particles possibly remained in the filtered solution and necessitated correction for scattering by fine particles (Babin *et al*., 2003). $OD_{\mathrm{S}(\lambda)}$ is the optical density for a specific band, while $OD_{(\mathrm{null})}$ is the average optical density over 740–750 nm; hence, the absorbance of CDOM can be assumed to be zero (Babin *et al*., 2003; Zhang *et al*., 2007).

2.5 Spectral slope (*S*)

A CDOM absorption spectrum, $a_{\mathrm{CDOM}}(\lambda)$, can be expressed as an exponential function (Bricaud *et al*., 1981;

Babin *et al*., 2003):

$$a_{\mathrm{CDOM}}(\lambda_i) = a_{\mathrm{CDOM}}(\lambda_{\mathrm{r}})\exp[-S(\lambda_i - \lambda_{\mathrm{r}})] \quad (2)$$

where $a_{\mathrm{CDOM}}(\lambda_i)$ is the CDOM absorption at a given wavelength λ_i, $a_{\mathrm{CDOM}}(\lambda_{\mathrm{r}})$ is the absorption estimate at the reference wavelength λ_{r} (440 nm), and S is the spectral slope. S is calculated by fitting the data to a linear model over a wavelength range of 360–600 nm (S_1) or a nonlinear model over the spectral range of 300–500 nm (S_2), as suggested by Zepp and Schlotzhauer (1981) and Zhang *et al*. (2007). Different S values could result from various curve-fitting approaches and the spectral range considered (Babin *et al*., 2003; Binding *et al*., 2008; Astoreca *et al*., 2009), which in turn affects CDOM absorption simulation and composition interpretation (Babin *et al*., 2003; Twardowski *et al*., 2004).

For the present study, the variation introduced by the fitted spectral wavelength ranges in CDOM is illustrated in Fig. 2. Obviously, fitting with Equation (2) for various spectral wavelength ranges achieve different prediction results. Various fitting methods also cause discrepancies in S and predicted CDOM absorption (Twardowski *et al*., 2004; Zhang *et al*., 2007). Predicted and measured $a_{\mathrm{CDOM}}(440)$ resulted in overestimated $a_{\mathrm{CDOM}}(440)$ for the spectral range 360–600 nm (S_1) using linear fitting method (Fig. 2a). In contrast, Fig. 2b showed a better correlation with slope close to unity and intercept to zero for the spectral range 300–500 nm (S_2) using an exponential curve fitting method. Thus, all subsequent results and discussion are focused on this range (300–500 nm).

3 Results

3.1 Variability of water constituents

The water constituents in the three reservoirs were summarized in Table 1. The concentration of Chl-a ranged from 21.63 μg/L to 128.30 μg/L for the ECR (coefficient of variation, CV: 48.31%). Similar Chl-a concentration (CV: 58.26%) was observed for the MR during the three field surveys. Lower Chl-a concentration was found in the GR, with even more stable algal growing (CV: 40.15%). Likewise, the TSM concentrations were demonstrated in Table 1, and the GR exhibited larger variability (SD: 9.91; CV: 78.84%). The ISM concentrations indicated that mineral-suspended and organic matter made nearly equivalent contributions to the dry weight of the TSM in the water column for three reservoirs.

3.2 CDOM absorption characteristics

The statistically descriptive CDOM absorption features for the ECR (Fig. 3a), the GR (Fig. 3b), and the MR (Fig. 3c) are similar in shape but different in magnitude. The $a_{\mathrm{CDOM}}(440)$ indicated that a large variation exists among the samples collected in various seasons and different reservoirs (Figs. 4a–4j). The averaged $a_{\mathrm{CDOM}}(440)$ for the ECR was initially 0.58 ± 0.08 m^{-1} on May 5, increased to 1.52 ± 0.23 m^{-1} on May 24, then dropped slightly to 1.37 ± 0.17 m^{-1} on August 24, and finally

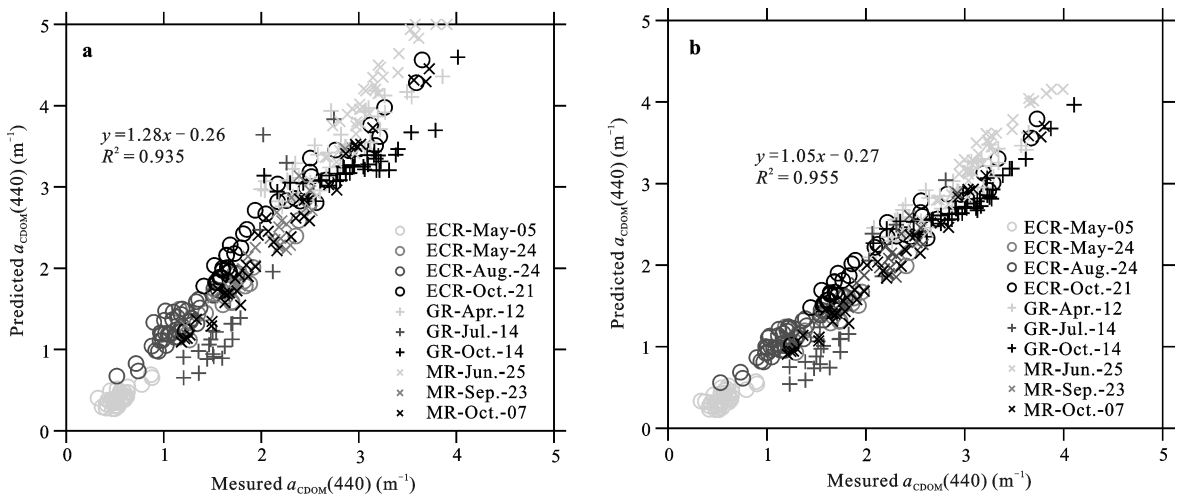

Fig. 2 Relationship between measured and predicted $a_{\mathrm{CDOM}}(440)$ values derived from fitting spectral ranges. a, S_1(360–600 nm) with linear regression method; and b, S_2(300–500 nm) with exponential regression method. ECR, Eagle Creek Reservoir; GR, Geist Reservoir; MR, Morse Reservoir

Table 1 Statistics for various water quality constituents

Dataset	Parameter (unit)	Min	Max	Average	SD	CV (%)
ECR	Chl-a (μg/L)	21.63	128.30	54.77	26.46	48.31
GR		0.24	62.33	33.97	13.64	40.15
MR		1.89	143.74	59.95	34.89	58.26
Combined		0.24	143.74	49.92	27.88	55.85
ECR	TSM (mg/L)	5.83	36.17	13.31	6.37	48.86
GR		5.17	81.17	12.57	9.91	78.84
MR		6.67	30.33	17.16	5.85	34.09
Combined		5.17	81.17	14.15	7.69	54.35
ECR	ISM (mg/L)	0.00	23.33	6.09	5.39	88.51
GR		0.00	70.00	5.85	9.59	163.93
MR		0.00	22.67	8.86	6.21	70.09
Combined		0.21	70.00	6.19	7.33	118.42
ECR	DOC (mg/L)	4.21	5.14	4.62	0.20	4.33
GR		3.74	4.86	4.20	0.28	6.67
MR		3.93	5.20	4.36	0.39	8.94
ECR	TOC (mg/L)	5.37	9.39	6.44	0.80	12.42
GR		4.42	10.33	6.28	1.19	18.95
MR		4.55	7.69	5.70	0.96	16.84

Notes: Chl-a, chlorophyll-a, TSM, total suspended matter, ISM, inorganic suspended matter, DOC, dissolved organic carbon, TOC, total organic carbon (both DOC and TOC were measured from samples collected on September 6, 2005, while other parameters were determined with samples collected in 2010); Min, minimum value; Max, maximum value; SD, standard deviation; CV, coefficient of variation (SD/average in percent). ECR, Eagle Creek Reservoir; GR, Geist Reservoir; MR, Morse Reservoir

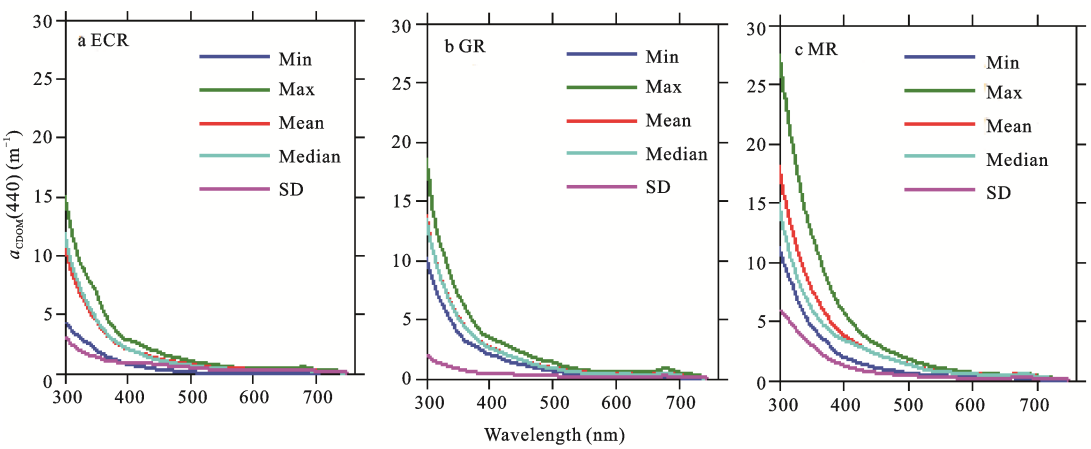

Fig. 3 Descriptive colored dissolved organic matter (CDOM) absorption spectra where wavelength is plotted vs. $a(\lambda)$. a, Eagle Creek Reservoir (ECR), b, Geist Reservoir (GR); c, Morse Reservoir (MR)

increased to 1.97 ± 0.47 m^{-1} on October 21. Higher averaged $a_{CDOM}(440)$ was observed for the GR on April 12 (3.23 ± 0.14 m^{-1}), decreased to 1.72 ± 0.21 m^{-1} on July 14, and dropped slightly to 1.50 ± 0.26 m^{-1} on October 14 (Figs. 4e–4g). The $a_{CDOM}(440)$ variability for the MR is illustrated in Figs. 4h–4j, a high average a_{CDOM} (440) (3.08 ± 0.38 m^{-1}) was observed for the samples collected on June 25. This average decreased to 1.91 ± 0.20 m^{-1} on September 23, and similar value (1.98 ± 0.46 m^{-1}) was found on October 7. As shown in Fig. 5a, significant differences were found between the ECR and the GR (F = 103.6, $p < 0.0001$) and the ECR and the MR (F = 151.4, $p < 0.0001$), though still significant, the level was reduced between the GR and the MR (F = 6.7, $p < 0.01$).

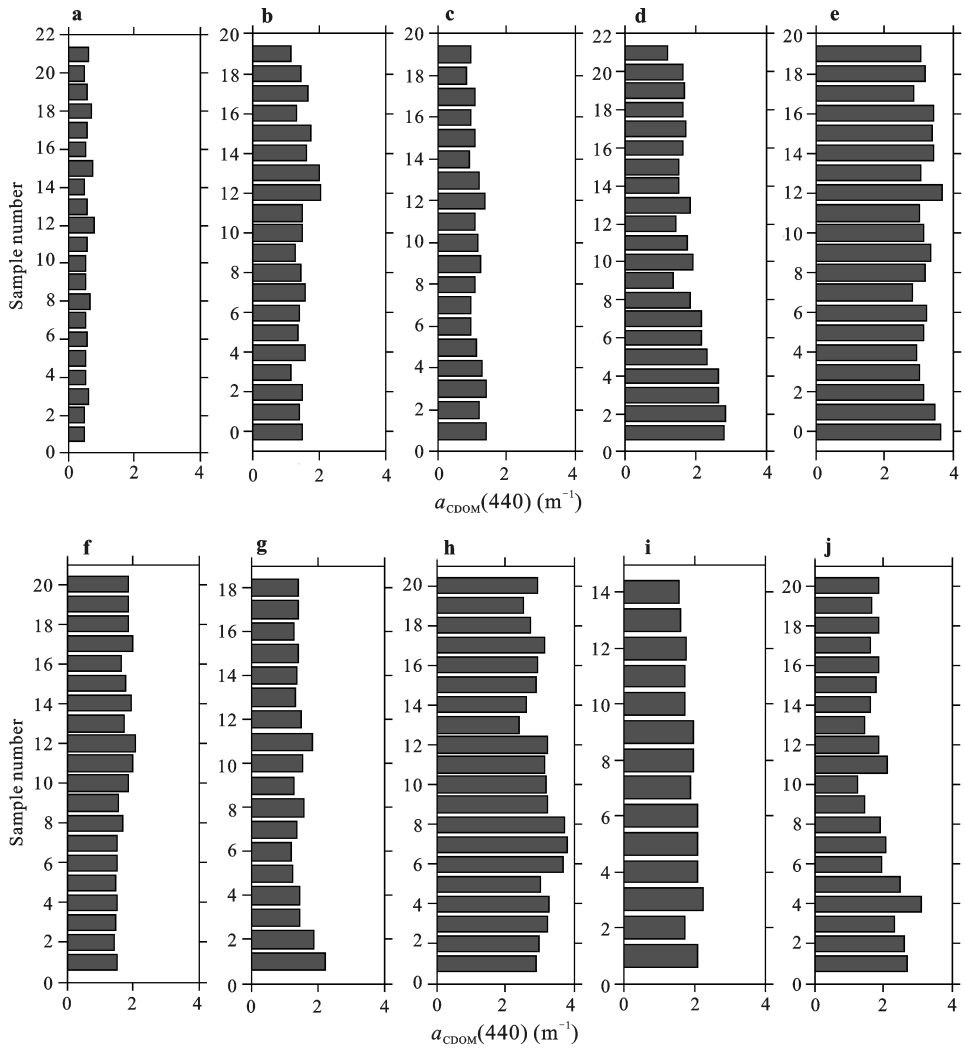

Fig. 4 $a_{CDOM}(440)$ variability for three reservoirs during different field surveys. a–d, $a_{CDOM}(440)$ for ECR on May 5, May 24, August 24 and October 21, respectively; e–g, $a_{CDOM}(440)$ for GR on April 12, July 14, and October 14, respectively; h–j, $a_{CDOM}(440)$ for MR on June 25, September 23 and October 7, respectively

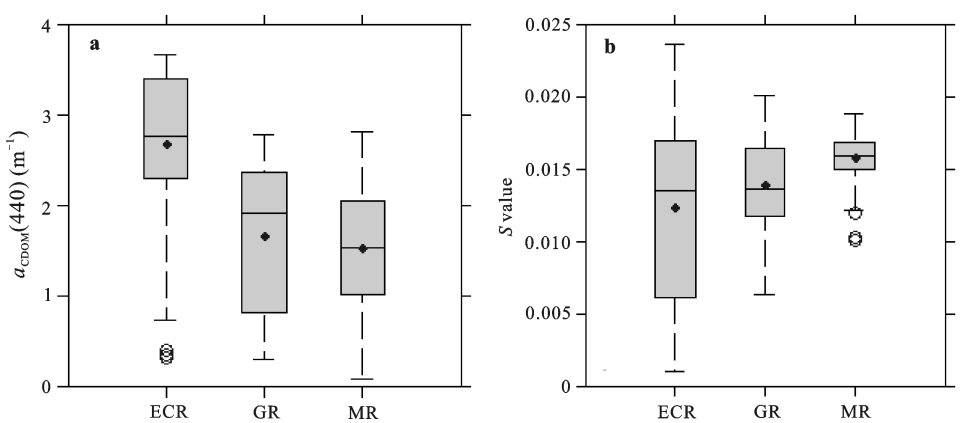

Fig. 5 Box plots of $a_{CDOM}(440)$ and S values for three reservoirs. ECR, Eagle Creek Reservoir; GR, Geist Reservoir; MR, Morse Reservoir. Black line and blue filled circles represent the median and mean respectively. Horizontal edges of the boxes denote the 25th and 75th percentiles; the whiskers denote the 10th and 90th percentiles and the blue circles represent outliers

3.3 Spectral slope (*S*) variation

The *S* values for field survey on May 5 (spring) showed higher average and small variation in the ECR (Table 2, Fig. 5b). It had comparatively small amplitude for the May 24 samples with larger variation. A comparable amplitude and variation of *S* values was observed on the third survey to that for the first survey, and the *S* values for last survey showed comparable amplitude with that for the second field survey (Table 2). Large variation for *S* value was observed for the ECR (CV: 7.21%–14.77%). Similarly, the *S* values for the GR showed large variation for the field survey on April 12 (spring following a strong watershed inflow event), with an average of 0.0136 nm^{-1} (Table 2). While the *S* exhibited a relatively small range (0.0102–0.0134 nm^{-1}) for field survey on July 14, and even smaller *S* values were observed for field survey on October 14. The *S* values for the MR exhibited a smaller variation among various stations and field surveys (Table 2). As shown in Fig. 5b, the *S* values for the ECR exhibit large variation with respect to the GR and the MR. Significant difference is observed between the ECR and the GR ($F = 6.8$, $p < 0.01$), likewise, even more significant difference between the ECR and the MR ($F = 40.3$, $p < 0.0001$), and the GR and the MR ($F = 31.8$, $p < 0.0001$) are exhibited.

3.4 Relationship between *S* and CDOM

The relationships between $a_{CDOM}(440)$ and *S* for each field survey are summarized in Table 3. The relationship varied significantly as indicated by the coefficient of determination ($0.082 < R^2 < 0.870$) and significance levels (p). As shown in Fig. 6, an inverse trend between $a_{CDOM}(440)$ and *S* can be observed for the three reservoirs. The *S* value for the first field survey over the ECR exhibited a strong negative linear correlation with $a_{CDOM}(440)$. A higher correlations between *S* and $a_{CDOM}(440)$ were observed for the ECR field surveys on August 24 ($R^2 = 0.870$, $p < 0.0001$) and October 21 ($R^2 = 0.673$, $p < 0.0001$), when low inflow and high algae exhibited. With a linear regression model, an R^2 of 0.553 was obtained for the GR field survey conducted on April 12 (spring), which is comparable to that for the ECR survey on May 5. A low correlation between *S* and $a_{CDOM}(440)$ was found for the GR survey on July 14 (summer), which could be mainly attributed to the fact that the CDOM composition of the frozen samples may have been changed. The strongest relationship ($R^2 = 0.778$, $p < 0.0001$) between *S* and $a_{CDOM}(440)$ was achieved for the GR survey on October 14 (autumn). Higher correlations obtained for three MR surveys on June 25 (summer; $R^2 = 0.787$), September 23 (autumn; $R^2 = 0.792$), and October 7 (autumn; $R^2 = 0.771$) with p-values all less than 0.0001.

Inverse relationships between *S* and a_{CDOM} in both open ocean water and coastal or inland water have been previously reported (Vodacek *et al*., 1997; Stedmon and Markager, 2001; Kowalczuk *et al*., 2006; Binding *et al*., 2008; Spencer *et al*., 2012). The *S* versus $a_{CDOM}(440)$ plot showed an inverse relationship for the aggregated dataset (Fig. 6), where most of the samples can be well fitted by a power equation ($S = 0.013 \times a_{CDOM}^{-0.42}$, $R^2 = 0.612$, $F = 125.7$, $p < 0.0001$), except for the field survey conducted across the GR on April 12 and across the MR on June 25, 2010. As suggested by Stedmon and Markager (2001), caution must be taken when studying the behavior of *S* in natural waters since it is highly sensitive to the wavelength range over which it is estimated (Babin *et al*., 2003; Zhang *et al*., 2007).

Table 2 Statistics of spectral slope (*S*) for three reservoirs on different sampling dates

Reservoir	Date	Min (nm^{-1})	Max (nm^{-1})	Mean (nm^{-1})	SD	CV (%)
ECR	2010-05-05	0.0175	0.0239	0.0201	0.0014	7.21
	2010-05-24	0.0072	0.0116	0.0089	0.0013	14.77
	2010-08-24	0.0115	0.0170	0.0141	0.0016	11.01
	2010-10-21	0.0083	0.0111	0.0097	0.0008	8.23
GR	2010-04-12	0.0117	0.0175	0.0136	0.0013	9.52
	2010-07-14	0.0102	0.0134	0.0115	0.0009	7.54
	2010-10-14	0.0074	0.0095	0.0083	0.0006	7.13
MR	2010-06-25	0.0115	0.0133	0.0125	0.0005	4.16
	2010-09-23	0.0092	0.0110	0.0098	0.0006	5.68
	2010-10-07	0.0085	0.0125	0.0100	0.0009	8.52

Table 3 Relationship between spectral slope value (S), and $a_{C\text{-}DOM}(440)$ of each field survey for three reservoirs

Reservoir	Date	n	R^2	F-statistic	p-value**
ECR	2010-05-05	21	0.271	3.93	< 0.05
	2010-05-24	20	0.583	27.51	< 0.0001
	2010-08-24	20	0.870	272.76	< 0.0001
	2010-10-21	20	0.673	79.82	< 0.0001
GR	2010-04-12	20	0.553	46.31	< 0.0001
	2010-07-14	20	0.082	4.09	< 0.05
	2010-10-14	23	0.778	77.89	< 0.0001
MR	2010-06-25	20	0.787	148.82	< 0.0001
	2010-09-23	14	0.792	100.02	< 0.0001
	2010-10-07	20	0.771	130.50	< 0.0001

Note: ** indicates at significant level 0.01

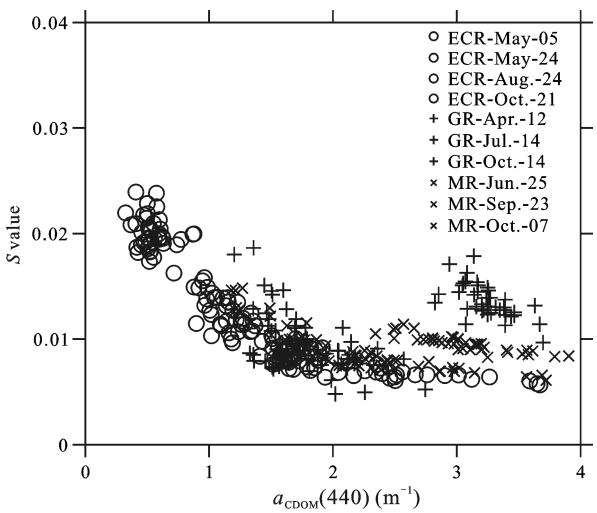

Fig. 6 Relationship between spectral slope (S) and $a_{CDOM}(440)$ for aggregated dataset

3.5 CDOM sources

In the present study, the correlation between $a_{CDOM}(440)$ and various optically active components (OACs), including Chl-a concentration, TSM concentration, and ISM concentration are presented in Table 4. The TSM concentration shows good correlation with CDOM for each field survey. However, we prefer using ISM concentration as the major proxy to indicate terrigenous CDOM sources due to phytoplankton being excluded. The $a_{CDOM}(440)$ had a significant positive correlation with ISM concentration ($R^2 = 0.313$, $p < 0.001$) and no significant correlation with Chl-a concentration ($R^2 = 0.017$, $p < 0.5$) for the ECR field survey on May 5. Actually, the ECR already exhibits cyanobacteria (Fig. 7a), due to the time lag between decomposed DOM substance and algal abundance, a loose correlation between CDOM and Chl-a concentration is shown. Significant positive correlations of $a_{CDOM}(440)$ with ISM concentration ($R^2 = 0.231$, $p < 0.05$) and Chl-a concentration ($R^2 = 0.312$, $p < 0.01$) suggested that both autochthonous and terrigenous CDOM contribute in this system on May 24, and that these may covary with CDOM (Fig. 7a). A similar trend can be found for the field survey on August 24 and October 21 across the ECR, but with higher correlation coefficients for both ISM concentrations ($R^2 = 0.344$, $p < 0.001$; $R^2 = 0.642$, $p < 0.0001$) and Chl-a concentration ($R^2 = 0.518$, $p < 0.001$; $R^2 = 0.763$, $p < 0.0001$).

Likewise, close association was observed between $a_{CDOM}(440)$ and ISM ($R^2 = 0.786$, $p < 0.0001$) for the GR on April 12 (Table 4). Cyanobacterial abundance

Table 4 Correlation between $a_{CDOM}(440)$ and concentrations of Chl-a, TSM, and ISM for each field survey

Reservoir	Date	n	Chl-a		TSM		ISM		Discharge (m^3/s)
			R^2	$p <$	R^2	$p <$	R^2	$p <$	
ECR	2010-05-05	21	0.017	0.5	0.372	0.001	0.313	0.01	1.43
	2010-05-24	20	0.312	0.01	0.411	0.001	0.231	0.05	4.43
	2010-08-24	20	0.518	0.001	0.517	0.0001	0.344	0.001	0.27
	2010-10-21	20	0.763	0.0001	0.693	0.0001	0.642	0.0001	0.13
GR	2010-04-12	20	0.013	0.9	0.210	0.01	0.786	0.0001	7.62
	2010-07-14	20	0.351	0.005	0.154	0.01	0.238	0.01	6.30
	2010-10-14	23	0.420	0.005	0.547	0.0001	0.314	0.005	1.08
MR	2010-06-25	20	0.081	0.8	0.713	0.0001	0.472	0.001	33.75
	2010-09-23	14	0.624	0.0001	0.576	0.0001	0.641	0.0001	0.13
	2010-10-07	20	0.587	0.0001	0.532	0.0001	0.432	0.001	0.08

Notes: Chl-a, chlorophyll-a; TSM, total suspended matter; and ISM, inorganic suspended matter. Discharge value indicates the 10-day average values before each of sampling campaign

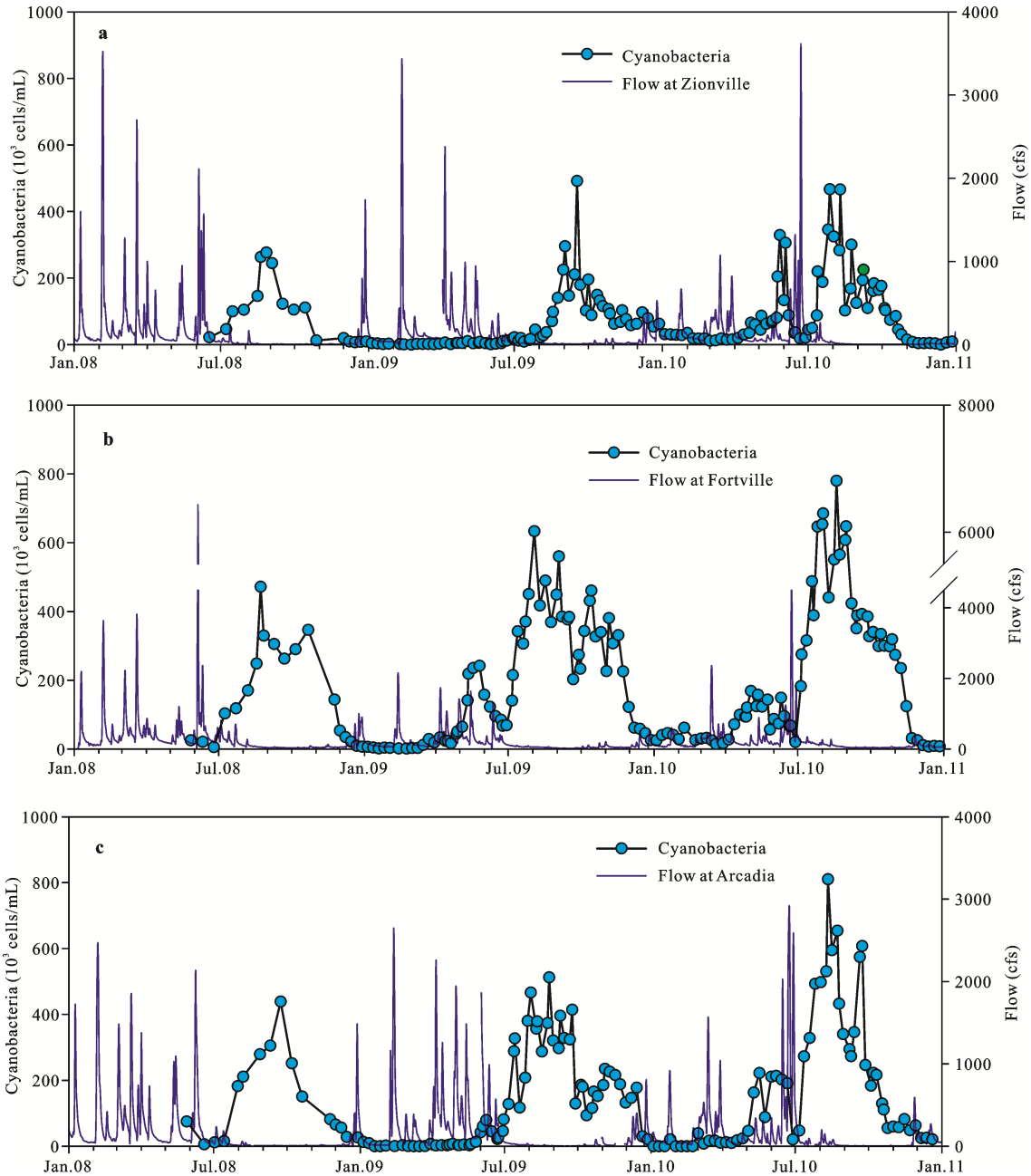

Fig. 7 Major watershed inflows for three reservoirs measured from stream gages on main inflowing stream (the data were collected by US Geological Survey gaging stations, starting from January 2008 to January 2011; cfs represents cubic foot per second) and phytoplankton biovolume dynamics. a, Eagle Creek Reservoir; b, Morse Reservoir; c, Geist Reservoir

was low (Fig. 7b), but snow melting and spring rainfall carried a large amount of DOC when runoff passed over bare soils (Table 4). Thaw in spring also played an important role in DOC releasing from soil or litter (Jaffe *et al.*, 2008; Agren *et al.*, 2010). The correlation between $a_{CDOM}(440)$ and Chl-a concentration (R^2 = 0.351, $p < 0.005$) is more significantly positive than that between $a_{CDOM}(440)$ and ISM ($R^2 = 0.238$, $p < 0.01$) for samples collected on July 14, 2010.

For the MR, a stronger correlation was observed between $a_{CDOM}(440)$ and ISM ($R^2 = 0.472$, $p < 0.001$) than between $a_{CDOM}(440)$ and Chl-a concentration (R^2 = 0.081, $p < 0.8$) for the early summer field survey (June 25), a stronger correlations of $a_{CDOM}(440)$ to ISM concentration ($R^2 = 0.641$, $p < 0.0001$) and to Chl-a concentration ($R^2 = 0.624$, $p < 0.0001$) on September 23,

and then almost equal correlation between $a_{CDOM}(440)$ and ISM concentration (R^2 = 0.432, p < 0.001) and Chl-a (R^2 = 0.587, p < 0.0001) in early autumn (September 23). A thunderstorm occurred on June 23 before the first field survey was conducted across the MR (Fig. 7c), and a large amount of runoff flushed soil organic and other organic compounds into the MR, resulting in stronger correlation of $a_{CDOM}(440)$ with ISM concentration than with Chl-a concentration (Table 4).

Considering the aggregated dataset, $a_{CDOM}(440)$ exhibits a significant positive correlation with ISM concentration (R^2 = 0.447, F = 87.4, p < 0.001) but not with Chl-a concentration (R^2 = 0.024, F = 6.7, p < 0.9) (Fig. 8). The autochthonous source contributed part of the CDOM in the three reservoirs (Table 4), but no significant correlation can be observed for $a_{CDOM}(440)$ and Chl-a concentration with the aggregated dataset (Fig. 8a) due to the punctuated nature of the inflows and seasonality of algal growing status (Fig. 7). However, a positive correlation (R^2 = 0.527, F = 117.1, p < 0.0001) was observed between $a_{CDOM}(440)$ and Chl-a concentration when excluded datasets from the ECR on May 5, the GR on April 12 and the MR on June 25.

4 Discussion

4.1 Spatial variation of CDOM

From a landscape perspective, CDOM concentration in lakes or reservoirs is considered to reflect terrestrial landscape source (Larson *et al*., 2007; Jaffe *et al*., 2008; Wilson and Xenopoulos, 2009; Agren *et al*., 2010), or autochthonous production from phytoplankton (Astoreca *et al*., 2009; Zhang *et al*., 2010; 2011a). As a result, hydro-climatic conditions of a catchment and water body primary productivity both affect CDOM dynamics, in addition to DOM chemical and photobleaching process (Hu *et al*., 2006; Helms *et al*., 2008; 2013b; Astoreca *et al*., 2009). It can be seen from Fig. 2, Fig. 4 and Fig. 5 that the MR shows higher CDOM than the GR and ECR, which might result from the high agricultural land use and landscape structure (Larson *et al*., 2007; Jaffe *et al*., 2008; Fellman *et al*., 2011). Our data, however, can not explain the differences among three reservoirs due to the surveys being not conducted simultaneously. Total organic carbon (TOC) and DOC data collected in September 6, 2005 indicated that no obvious difference existed for the three reservoirs, but did show a large CV for the MR (Table 1), which is consistent with CDOM absorption characteristic for the MR. Given the low discharge in September (Fig. 7), the capacity of streams to carry terrestrial CDOM is limited, which may not explain the landscape impact on CDOM variation for the three reservoirs for the data collected in 6 September 2005.

4.2 Temporal dynamics of CDOM

The CDOM is originated from both allochthonous and autochthonous sources. The composition of CDOM affects its absorptions features. Allochthonous source is generally dominated by large molecular DOM compound. As shown in Fig. 4, higher $a_{CDOM}(440)$ is mainly observed in punctuated discharge events, e.g., April 12 over the GR and June 25 over the MR. Changes in the CDOM composition may be attributed to photo-oxida-

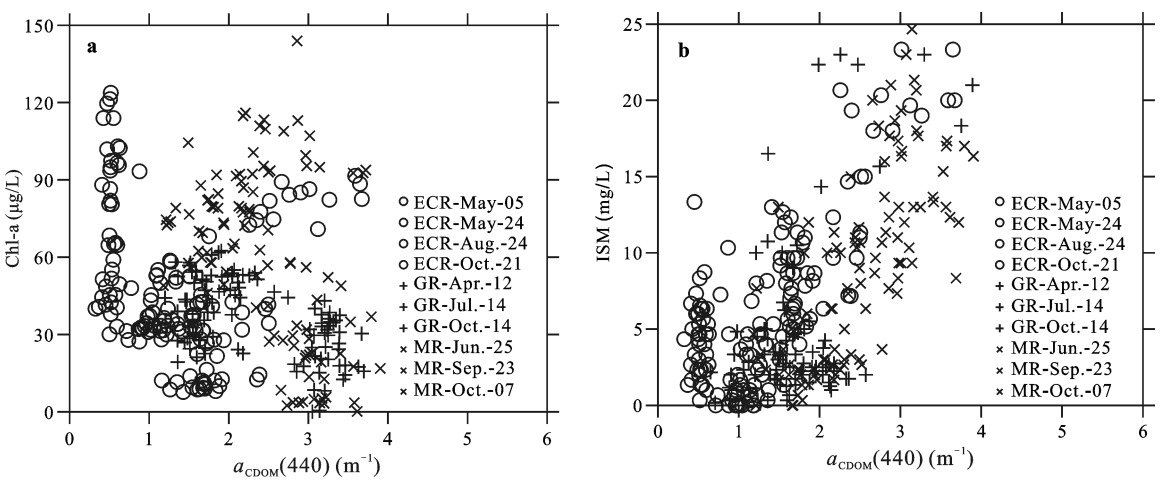

Fig. 8 Relationship of $a_{CDOM}(440)$ with chlorophyll-a concentration (a) and inorganic suspended matter (ISM) concentration (b)

tion (Vodacek *et al*., 1997; Miller *et al*., 2009; Spencer *et al*., 2009; Goldman *et al*., 2013), selective absorption of DOM onto mineral sediments (sorptive fractionation), as well as seasonal and dynamic biological activities (Wetzel, 2001; Binding *et al*., 2008), e.g., phytoplankton community building and seasonality (Tedesco and Clercin, 2011). These activities result from the presence of phytoplankton-derived CDOM further processed by bacteria and/or by photo-oxidation (Binding *et al*., 2008; Jaffe *et al*., 2008; Zhang *et al*., 2009; 2011b). The interaction between allochthonous and autochthonous CDOM also complicates the situation for inland waters (Twardowski *et al*., 2004; Larson *et al*., 2007; Jaffe *et al*., 2008; Zhang *et al*., 2010). Inflow discharge is the major factors that control DOM concentration (Larson *et al*., 2007; Jaffe *et al*., 2008; Agren *et al*., 2010; Spencer *et al*., 2012), coupled with phytoplankton growing pattern that determines the CDOM temporal dynamics in algal blooming seasons (Zhang *et al*., 2011a; 2011b).

4.3 Spatio-temporal dynamics of *S*

The *S* for all sampling stations fell into the range of 0.0750–0.0250 nm^{-1}, as reported by Markager and Vincent (2000). However, this value is lower than that derived from the Erie Lake (average = 0.0161 nm^{-1}) reported by Binding *et al*. (2008), and the Taihu Lake (average = 0.0144 nm^{-1}) reported by Zhang *et al*. (2007). Some of the differences is likely due to varying fitting methods used or spectral ranges considered (Babin *et al*., 2003; Twardowski *et al*., 2004). The other possibility is the high algal abundance in the three reservoirs (Chl-a concentrations ranging from 0.24 μg/L to 143.74 μg/L with an average of 49.92 μg/L) and high terrestrial DOC source concentration due to high percentage of agricultural land use (above 60%), which might change the CDOM composition (Jaffe *et al*., 2008; Spencer *et al*., 2009; 2012).

Based on the data distribution in Fig. 6, it can be seen that the proportion of terrigenous DOM is in good accordance with the highest CDOM concentration of $a_{CDOM}(440) \geq 3.0\ m^{-1}$ and the lowest *S* value of 0.07 nm^{-1}. The short exposure time to solar radiation may explain the relative lower *S* value due to the high molecular weight dominating the CDOM component (De Haan and De Boer, 1987; Carder *et al*., 1989; Helms *et al*., 2008; Astoreca *et al*., 2009). The high watershed inflow into the MR on June 25 before sampling date (Fig. 7c and Table 4) resulted in elevated terrigenous CDOM concentrations and may explain the distinct correlation between *S* and $a_{CDOM}(440)$ absorption in spring when watershed inflow events are more common and abundant, this is in agreement with Spencer *et al*. (2008; 2012) that runoff affect lake entrophic status and algal growing, affecting the CDOM components.

4.4 Source analysis of CDOM

For inland waters, CDOM mainly originates from terrigenous sources, particularly from river or stream discharges, whereas the remaining portion is autochthonous (Hood *et al*., 2003; Jaffe *et al*., 2008; Spencer *et al*., 2008; 2012). The three reservoirs are usually dominated by discharge suspensions carrying sediments eroded from agricultural land or re-suspended sediments by showing high correlation with the ISM concentration for the aggregated dataset (Fig. 8b). Watersheds associated with rivers have been suggested to play important roles in determining CDOM quantity and quality (Larson *et al*., 2007; Sobek *et al*., 2007; Helms *et al*., 2008; Jaffe *et al*., 2008; Spencer *et al*., 2009; 2012; Agren *et al*., 2010; Zhang *et al*., 2011a). Considering the pulsed discharge rates from tributaries for these three reservoirs (Tedesco and Clercin, 2011), the contribution of these tributaries to CDOM in the reservoirs appears to have significant variation (Fig. 7). The selective absorption of DOM may have possibly caused cohesion among mineral sediments (Kaiser and Zech, 1999; Wetzel, 2001; Binding *et al*., 2008). Another interesting fact revealed in this work is that *S* is more varied for inland waters due to the terrigenous DOM sources carried by stream discharge (Spencer *et al*., 2009; Agren *et al*., 2010; Fellman *et al*., 2011). It is also worth noting that CDOM from phytoplankton decomposition may play an important role as revealed by the close relationship between CDOM and Chl-a concentration (Fig. 8a and Table 4) during phytoplankton biomass abundant period, which is consistent with the finding for eutrophic waters, i.e., the Taihu Lake and waters from the Yunnan Guizhou Plateau from China (Zhang *et al*., 2009; 2011b). It was worth noting that two peaks of biovolume taken place during May and October, and high inflows generally resulted in low biovolume due to the dilution effect. This suggests an autochthonous CDOM dominated system for the survey conducted on July 14 although a relative high inflow exhibited before sampling for the GR (Fig. 7b and Table 4). The association between $a_{CDOM}(440)$

and ISM concentration (R^2 = 0.314, p < 0.005) and Chl-a concentration (R^2 = 0.420, p < 0.005) on October 14. A positive correlation (R^2 = 0.533, F = 117.1, p < 0.0001) was observed between CDOM and Chl-a concentration when excluded datasets from the ECR on May 5, the GR on April 12 and the MR on June 25, suggesting that autochthonous CDOM play an important role during algal blooming months (Zhang *et al*., 2009).

5 Conclusions

Based on *in situ* measurements and laboratory analyses, the CDOM absorption property of productive waters in the central Indiana was systematically investigated. The results show that terrigenous DOM is responsible for the low spectral slope *S*, which is mainly attributed to a high-molecular weight humic acid proportion. Hydro-climatic conditions control this process, and inflow from watersheds plays an important role for early spring CDOM concentration and components. In late summer and autumn, a long period of low watershed inputs and less rainfall causes reduced water-soil losses from the upstream and CDOM is influenced mainly by phytoplankton decomposition, and accumulation due to long water residence time during this portion of the year is another factor for the high concentration of CDOM in the three reservoirs. The results indicate that CDOM for the three reservoirs is generally low except watershed inflow events occur. The phenomenon of the periodical co-variation of CDOM with phytoplankton or ISM was observed. The co-variation linkage between CDOM and phytoplankton gradually increases from summer, decreases in mid-autumn. The CDOM source analysis for this study is still far from being solved, the fluorescence excitation-emission matrix spectroscopy (EEMs) can provide abundant information of CDOM characteristics. In the ongoing work, we will focus on CDOM source tracing through EEMs as its promising potentials for characterizing the composition of fluorophores given its high selectivity and sensitivity to CDOM in water columns.

Acknowledgments

The authors would like to thank all the participants for the laboratory analysis of CDOM and DOC concentration from water samples. Field data were collected with the capable assistance of Robert E Hall from the Department of Earth Sciences and Center for Earth and Environmental Science, Indiana University-Purdue University, Indianapolis. Many thanks also go to three anonymous reviewers for their valuable comments that really strengthened our manuscript.

References

Agren A, Haei M, Kohler S J *et al*., 2010. Regulation of stream water dissolved organic carbon (DOC) concentrations during snowmelt; the role of discharge, winter climate and memory effects. *Biogeosciences*, 7: 2901–2913. doi: 10.5194/bg-7-2901-2010

Arar E J, Collins G B, 1997. U.S. Environmental Protection Agency Method 445.0, In vitro determination of chlorophyll *a* and pheophytin a in marine and freshwater algae by fluorescence, revision 1.2: Cincinnati, Ohio, U.S. Environmental Protection Agency National Exposure Research Laboratory, Office of Research and Development.

Astoreca R, Rousseau V, Lancelot C, 2009. Colored dissolved organic matter (CDOM) in Southern North Sea waters: Optical characterization and possible origin. *Estuarine Coastal and Shelf Science*, 85(4): 633–640. doi: 10.1016/j.ecss.2009.10.010

Babin M, Stramski D, Ferrari G M *et al*., 2003. Variations in the light absorption coefficients of phytoplankton, nonalgal particles, and dissolved organic matter in coastal waters around Europe. *Journal of Geophysical Research*, 108(C7): 3211. doi: 10.1029/2001JC000882

Binding C E, John H J, Bukata R P *et al*., 2008. Spectral absorption properties of dissolved and particulate matter in Lake Erie. *Remote Sensing of Environment*, 112(4): 1702–1711. doi: 10.1016/j.rse.2007.08.017

Bricaud A, Morel A, Prieur L, 1981. Absorption by dissolved organic matter of the sea (yellow substance) in the UV and visible domain. *Limnology and Oceanography*, 26(1): 43–53. doi: 10.4319/lo.1981.26.1.0043

Brown M, 1977. Transmission spectroscopy examinations of natural waters: C. Ultraviolet spectral characteristics of the transition from terrestrial humus to marine yellow substance. *Estuarine and Coastal Marine Science*, 5(3): 309–317. doi: 10.1016/0302-3524(77)90058-5

Busse L B, Gunkel G, 2001. Riparian alder fens—Source or sink for nutrients and dissolved organic carbon?—1. Effects of water level fluctuations. *Limnologica*, 31(4): 307–315. doi: 10.1016/S0075-9511(01)80033-5

Carder K L, Steward R G, Harvey R G *et al*., 1989. Marine humic and fulvic acids: Their effects on remote sensing of ocean chlorophyll. *Limnology and Oceanography*, 34(1): 68–81. doi: 10.4319/lo.1989.34.1.0068

Cory N, Buffam I, Laudon H *et al*., 2006. Landscape control of stream water aluminum in a boreal catchment during spring flood. *Environmental Science and Technology*, 40(11): 3494–3500. doi: 10.1021/es0523183

De Haan H, De Boer T, 1987. Applicability of light absorbance

and fluorescence as measures of concentration and molecular size of dissolved organic carbon in humic Laken Tjeukemeer. *Water Research*, 21(6): 731–734. doi: 10.1016/0043-1354(87)90086-8

Fellman J B, Petrone K C, Grierson F, 2011. Source, biogeochemical cycling, and fluorescence characteristics of dissolved organic matter in an agro-urban estuary. *Limnology and Oceanography*, 56(1): 243–256. doi: 10.4319/lo.2011.56.1.0243

Fichot C G, Benner R, 2011. A novel method to estimate DOC concentrations from CDOM absorption coefficients in coastal waters. *Geophysical Research Letter*, 38(3): L03610. doi: 10.1029/2010GL046152

Goldman E A, Smith E M, Richardson T L, 2013. Estimation of chromophoric dissolved organic matter (CDOM) and photosynthetic activity of estuarine phytoplankton using a multiple-fixed-wavelength spectral fluorometer. *Water Research*, 47(4): 1616–1630. doi: 10.1016/j.watres.2012.12.023

Helms J R, Mao J, Schmidt-Rohr K *et al*., 2013a. Photochemical flocculation of terrestrial dissolved organic matter and iron. *Geochimica Cosmochimica Acta*, 121(15): 398–413. doi: 10.1016/j.gca.2013.07.025

Helms J R, Stubbins A, Perdue E M *et al*., 2013b. Photochemical bleaching of oceanic dissolved organic matter and its effect on absorption spectral slope and fluorescence. *Marine Chemistry*, 155: 81–91. doi: 10.1016/j.marchem.2013.05.015

Helms J R, Stubbin A, Ritchie J D *et al*., 2008. Absorption spectral slopes and slope ratios as indicators of molecular weight, source, and photobleaching of chromophoric dissolved organic matter. *Limnology and Oceanography*, 53(3): 955–969. doi: 10.4319/lo.2008.53.3.0955

Hood E W, Mcknight D M, Williams M W, 2003. Sources and chemical character of dissolved organic carbon across an alpine/subalpine ecotone, Green Lakes Valley, Colorado Front Range, United States. *Water Resources Research*, 39(7): 1188. doi: 10.1029/2002WR001738

Hu C M, Lee Z P, Muller-Karger F E *et al*., 2006. Ocean color reveals phase shift between marine plants and yellow substance. *IEEE Geoscience and Remote Sensing Letter*, 3(2): 262–266. doi: 10.1109/LGRS.2005.862527

Jaffe R, McKnight D, Maie N *et al*., 2008. Spatial and temporal variations in DOM composition in ecosystems: The importance of long-term monitoring of optical property. *Journal of Geophysical Research*, 113(G4): G04032. doi: 10.1029/2008JG000683

Kaiser K, Zech W, 1999. Release of natural organic matter sorbed to oxides and a subsoil. *Soil Science Society of American Journal*, 63(5): 1157−1166. doi: 10.2136/sssaj1999.6351157x

Kowalczuk P, Stedmon C A, Markager S, 2006. Modeling absorption by CDOM in the Baltic Sea from salinity and chlorophyll. *Marine Chemistry*, 101(1–2): 1–11. doi: 10.1016/j.marchem.2005.12.005

Larson J H, Frost P C, Zheng Z Y *et al*., 2007. Effects of upstream lakes on dissolved organic matter in streams. *Limnology and Oceanography*, 52(1): 60–69. doi: 10.4319/lo.2007.52.1.0060

Lee Z P, Carder K L, Arnone R A, 2002. Deriving inherent optical properties from water color: A multiband quasi-analytical algorithm for optically deep waters. *Applied Optics*, 41(27): 5755–5772. doi: 10.1364/AO.41.005755

Markager W, Vincent W F, 2000. Spectral light attenuation and absorption of UV and blue light in natural waters. *Limnology and Oceanography*, 45(3): 642–650. doi: 10.4319/lo.2000.45.3.0642

Miller M P, McKnight D M, Chapra S C *et al*., 2009. A model of degradation and production of three pools of dissolved organic matter in an alpine lake. *Limnology and Oceanography*, 54(6): 2213–2227. doi: 10.4319/lo.2009.54.6.2213

Morel A, Gentili B, 2009. A simple band ratio technique to quantify the colored dissolved and detrital organic material from ocean color remotely sensed data. *Remote Sensing of Environment*, 113: 998–1011. doi: 10.1016/j.rse.2009.01.008

Sobek S, Tranvik L J, Prairie Y T *et al*., 2007. Patterns and regulation of dissolved organic carbon: An analysis of 7500 widely distributed lakes. *Limnology and Oceanography*, 52(3): 1208–1219. doi: 10.4319/lo.2007.52.3.1208

Song K S, Li L, Tedesco L P *et al*., 2012. Hyperspectral determination of eutrophication for a water supply source via genetic algorithm-partial least squares (GA–PLS) modeling. *Science of Total Environment*, 426: 220–232. doi: 10.1016/j.scitotenv.2012.03.058

Song K, Liu D, Li L *et al*., 2010. Spectral absorption properties of colored dissolved organic matter (CDOM) and total suspended matter (TSM) of inland waters. *Proceedings of the International Society for Optical Engineering*, 7811: 78110B. doi: 10.1117/12.859634

Song K S, Li L, Tedesco L *et al*., 2013. Remote estimation of phycocyanin (PC) for inland waters coupled with YSI PC fluorescence probe. *Environmental Science and Pollution Research*, 20(8): 5330–5340. doi: 10.1007/s11356-013-1527-y

Spencer R G M, Aiken G R, Wickland K P *et al*., 2008. Seasonal and spatial variability in dissolved organic matter quantity and composition from the Yukon River Basin, Alaska. *Global Biogeochemical Cycling*, 22(4): GB4002. doi: 10.1029/2008GB003231

Spencer R G M, Butler K D, Aiken G R, 2012. Dissolved organic carbon and chromophoric dissolved organic matter properties of rivers in the U.S.A. *Journal of Geophysical Research*: *Biogeosciences*, 117(G3): G03001. doi: 10.1029/2011JG001928

Spencer R G M, Stubbins A, Hernes P J *et al*., 2009. Photochemical degradation of dissolved organic matter and dissolved lignin phenols from the Congo River. *Journal of Geophysical Research*, 114(G3): G03010. doi: 10.1029/2009JG000968

Stedmon C A, Markager S, 2001. The optics of chromophoric dissolved organic matter (CDOM) in the Greenland Sea: An algorithm for the differentiation between marine and terrestrially derived organic matter. *Limnology and Oceanography*, 46(8): 2087–2093. doi: 10.4319/lo.2001.46.8.2087

Stedmon C A, Markager S, Søndergaard M *et al*., 2006. Dissolved organic matter (DOM) export to a temperate estuary: Seasonal

variations and implications of land use. *Estuarine Coast*, 29(3): 388–400. doi: 10.1007/BF02784988

Sun J, Liu D, 2003. Geometric models for calculating cell biovolume and surface area for phytoplankton. *Journal of Plankton Research*, 25(11): 1331–1346. doi: 10.1093/plankt/fbg096

Tedesco L, Clercin N A, 2011. Algal ecology, cyanobacteria toxicity and secondary matebolites production of the three eutrophic drinking water supply and recreational use reservoirs in central Indiana. *2010 Research Project Final Report*, *Indianapolis*, 25–29.

Tranvik L J, Downing J A, Cotner J B *et al*., 2009. Lakes and reservoirs as regulators of carbon cycling and climate. *Limnology and Oceanography*, 54(6): 2298–2314. doi: 10.4319/lo.2009.54.6_part_2.2298

Twardowski M S, Boss E, Sullivan J M *et al*., 2004. Modeling the spectral shape of absorption by chromophoric dissolved organic matter. *Marine Chemistry*, 89(1–4): 69–88. doi: 10.1016/j.marchem.2004.02.008

Vodacek A, Blough N V, Degrandpre M D *et al*., 1997. Seasonal variation of CDOM and DOC in the Middle Atlantic Bight: Terrestrial inputs and photooxidation. *Limnology and Oceanography*, 42(4): 674–686. doi: 10.4319/lo.1997.42.4.0674

Wetzel R G, 2001. *Limnology*: *Lake and River Ecosystems* (3rd ed.). San Diego: Academic Press, 731–759.

Williamson C E, Rose K C, 2010. When UV meets fresh water. *Science*, 329(5992): 637–639. doi: 10.1126/science.1191192

Wilson H, Xenopoulos M A, 2009. Effects of agricultural land use on the composition of fluvial dissolved organic matter. *Nature Geoscience*, 2(1): 37–41. doi: 10.1038/ngeo391

Zepp R G, Schlotzhauer P F, 1981. Comparison of photo-chemical behavior of various humic substances in water. III. Spectroscopic properties of humic substances. *Chemosphere*, 10(5): 479–486. doi: 10.1016/0045-6535(81)90148-X

Zhang Y L, Qin B Q, Zhu G W *et al*., 2007. Chromophoric dissolved organic matter (CDOM) absorption characteristics in relation to fluorescence in Lake Taihu, China, a large shallow subtropical lake. *Hydrobiologia*, 581(1): 43–52. doi: 10.1007/s10750-006-0520-6

Zhang Y L, van dijk M K, Liu M L *et al*., 2009. The contribution of phytoplankton degradation to chromophoric dissolved organic matter (CDOM) in eutrophic shallow lakes: Field and experimental evidence. *Water Research*, 43(18): 4685–4697. doi: 10.1016/j.watres.2009.07.024

Zhang Y L, Zhang E L, Yin Y *et al*., 2010. Characteristics and sources of chromophoric dissolved organic matter in lakes of the Yungui Plateau, China, differing in trophic state and altitude. *Limnology and Oceanography*, 55(6): 2645–2659. doi: 10.4319/lo.2010.55.6.2645

Zhang Y L, Yin Y, Zhang E L *et al*., 2011a. Spectral attenuation of ultraviolet and visible radiation in lakes in the Yunnan Plateau, and the middle and lower reaches of the Yangtze River, China. *Photochemical and Photobiological Sciences*, 10(4): 469–482. doi: 10.1039/C0PP00270D

Zhang Y, Yin Y, Zhu G *et al*., 2011b. Characterizing chromophoric dissolved organic matter in Lake Tianmuhu and its catchment basin using excitation emission matrix fluorescence and parallel factor analysis. *Water Research*, 45(16): 5110–5122. doi: 10.1016/j.watres.2011.07.014